Method of determining the inherent viscosity of a slurry and other rheological trends as illustrated by a data bank of over 200 different slurries

A.D. Thomas
Slurry Systems Pty Limited, Sydney, Australia
allan@allanthomas.com.au

This paper argues that the viscosity of a slurry is made up of an inherent viscosity component and a mechanical interference component. The inherent viscosity is shown to be given by $\mu_{inh} = e^{(Atot\ -2.7)Vrtot}$ where Vr_{tot} is the Volume Ratio of total solids and A_{tot} is a constant for any particular slurry. The applicability of this equation is illustrated by specific test results for a number of sand-clay and wide size distribution slurries. Plastic viscosity results from a rheology data bank of tests on 201 different slurries are plotted against the p_{50} particle size and are shown to support the theory. Yield stress data for the same slurries are also presented.

1. INTRODUCTION

This paper is in two sections. The first section is concerned with the relevant viscosity to use in predicting turbulent, heterogeneous slurry flow behaviour. To logically apply the same methods as used with slurries for which the viscosity of the "vehicle" portion is easily identified, such as a sand-water slurry, the inherent viscosity of a slurry should be used. A method of determining the inherent viscosity of a wide size distribution viscous slurry is developed. The viscosity of interest is the Bingham plastic viscosity which is relevant to turbulent, heterogeneous flow prediction. In the current paper the plastic viscosity will generally be referred to simply as viscosity. The applicability of the method is illustrated by test results for a number of sand-clay slurries and also tests on wide size distribution slurries before and after screening out some coarser solids.

In the second part of the paper plastic viscosity data from a rheology data bank of 201 different slurries are plotted against the p_{50} particle size to support the theory. The rheology data bank is also used to examine Bingham yield stress trends and the relationship with plastic viscosity.

2. THE RELEVANT VISCOSITY FOR TURBULENT FLOW PREDICTION

2.1 Slurries for which the vehicle portion can easily be identified

The vast majority of slurry pipelines operate in turbulent flow and the two major hydraulic properties of interest are the pressure gradient and the deposit velocity. For coarse granular particles in water, such as a sand-water slurry, the known viscosity of water is used to

predict the turbulent flow pressure gradient and deposit velocity. Sometimes the sand may be carried in a Newtonian fluid of viscosity and density greater than water such as a brine solution. In this case the Newtonian viscosity of the brine is measured and used in turbulent flow heterogeneous predictions.

Next consider a slurry composed of a mixture of sand in a clay slurry. In this case viscometer tests would be conducted on the non-Newtonian clay slurry. In their analysis of non-Newtonian turbulent flow, Wilson and Thomas (1) assume a Bingham model with the plastic viscosity based on the high shear rate viscometer data and the yield stress being the extrapolation to the shear stress axis. The plastic viscosity fitted to the high shear rate viscometer data, equates to the shear viscosity at infinite shear rate, and would seem the appropriate viscosity to use to predict the deposit velocity of the sand-clay mixtures in turbulent flow.

For both the sand-brine and the sand-clay slurries, the turbulent flow pressure gradient and the deposit velocity would normally be predicted using a similar approach as for sand-water slurries, i.e. considering the sand in a brine (or clay) "vehicle" and using the brine (or clay) viscosity.

If the sand particles are fine, the sand-brine slurry or the sand-clay slurry may be sufficiently slow settling to enable viscometer tests on the mixture. As noted by the present author, Thomas (2), the measured viscosity increase of the brine (or the clay), will be approximated by the equation of D.G. Thomas (3), or a similar equation. The D.G. Thomas equation is shown in Eqn 1 where Cv is the volume concentration of solids in the slurry.

$$\mu_{slurry} / \mu_{fluid} = 1 + 2.5Cv + 10.05\, Cv^2 + 0.00273 \exp(16.6\, Cv) \qquad (1)$$

As noted above, the sand-brine (or sand-clay) turbulent flow pressure gradient and the deposit velocity would normally be predicted using a similar approach as for sand-water slurries, i.e. considering the sand in a brine (or clay) vehicle and using the brine (or clay) viscosity. Alternatively the measured mixture viscosity might be used to predict the pressure gradient but the viscosity of the brine (or clay) would still normally be used to predict the deposit velocity.

2.2 Continuous size distribution slurries

In the three examples considered above, there is no doubt what constitutes the "vehicle" portion of the slurry. For a sand-water slurry the vehicle is water, for a sand-brine slurry the vehicle is the brine, and for a sand-clay slurry the vehicle is the clay slurry. More typically, slurries contain a wide, continuous size distribution, in which case it is not so easy to decide what is the vehicle portion. Gillies and Shook (4) and Wilson et al (5) assume particles finer than 75 μm constitute the vehicle slurry, whereas Sellgren and Wilson (6) assume particles finer than 40 μm. These are somewhat arbitrary demarcations which also do not take into account any influence of solids SG on the demarcation size.

For the purposes of turbulent flow prediction, the present paper argues that the viscosity of a slurry is made up of an inherent viscosity component and a mechanical interference component. The inherent viscosity component is considered a property of the slurry even when the slurry is static. Thus for a sand-water slurry the inherent viscosity is the viscosity of water. Although it might be possible to measure the viscosity of the sand-water mixture in a vertical tube viscometer for example, the measured viscosity above that of water would be all due to mechanical interference and would not normally be used in turbulent flow predictions. The water viscosity is used instead. Similarly for a sand-brine slurry the

inherent viscosity is the viscosity of the brine. For the sand-clay slurry the inherent viscosity is considered to be the (plastic) viscosity of the clay slurry since the clay viscosity is dependant on fine particle attraction forces which exist even when the slurry is static. For turbulent flow prediction purposes the plastic viscosity of the clay slurry is the relevant viscosity. The additional viscosity due to the sand only occurs as a result of movement and mechanical interaction between the sand particles as per Eqn 1.

Most slurries have a wide size distribution and include some fine particles for which surface chemical effects are important. The measured viscosity of the slurry will consist of an inherent viscosity component and a mechanical interference component. Following the same logic as used above in relation to sand-water, sand-brine and sand-clay slurries, the mechanical interference component, although contributing to the viscosity, should not be used in turbulent flow predictions, at least for deposit velocity predictions, only the inherent portion should be used.

As an example, consider slurries of particle size suitable for long distance transportation which for concentrates means particle size typically less than 100 μm. The standard prediction procedure for these slurries is to measure the rheology using a rotational viscometer and determine the Bingham yield stress and plastic viscosity. The pressure gradient is predicted using the measured yield stress and plastic viscosity, as is the laminar-turbulent transition velocity. The plastic viscosity is normally used to predict the heterogeneous deposit velocity. But, assuming there is some mechanical interference component to the measured viscosity, and to be consistent with the previous approaches for sand-water, sand-brine and sand-clay slurries, only the inherent viscosity portion should be used to predict the heterogeneous deposit velocity rather than the full measured plastic viscosity. However it turns out that for most “long distance” slurries, the deposit velocity is controlled more by laminar-turbulent transition rather than heterogeneous deposition so the use of the measured viscosity rather than the inherent viscosity portion only is somewhat immaterial.

The situation changes when we consider a slurry slightly coarser than the normal “long distance” slurry. Recently the author was investigating the pumping of a magnetite slurry significantly coarser than the normal minus 100 μm magnetite currently pumped over long distances. A typical minus 100 μm magnetite slurry does not settle so fast as to prevent testing in a rotational viscometer. In contrast the coarser magnetite being investigated settled very fast making viscometer testing extremely difficult. It was obvious that there was a significant mechanical interference component to the measured viscosity. When it came to predicting the turbulent flow deposit velocity the question then arose as to whether the full measured viscosity was the relevant viscosity to use. This is in fact what led the author to investigate the idea of an inherent viscosity for prediction purposes, resulting in the present paper.

3. DETERMINING THE INHERENT VISCOSITY

3.1 Slurry viscosity components

The premise of this paper is that the inherent viscosity of a slurry is a property of the slurry even when the slurry is stationary. The measured viscosity will generally be higher than the inherent viscosity because of an additional viscosity component due to mechanical interference effects between particles when the slurry is in motion. The question is: How do we determine what is the inherent viscosity portion of the measured viscosity of a wide size distribution slurry?

3.2. Rheology measurement

Slurries containing fine or colloidal sized particles are non-Newtonian and are analysed in the current paper as Bingham plastics. They possess a yield stress and a plastic viscosity. The plastic viscosity equals the viscosity at infinite shear rate and can be considered the relevant viscosity for turbulent flow prediction. Figure 1 shows typical rheograms obtained by the author in a Contraves RM115, narrow gap rotational cylindrical viscometer, bob diameter 45.62 mm, cup diameter 48.20 mm, diameter ratio 0.9465. The straight line fitted to the high shear rate data represents the Bingham curve. The intercept on the shear stress axis is the Bingham yield stress and the slope of the line is the plastic viscosity.

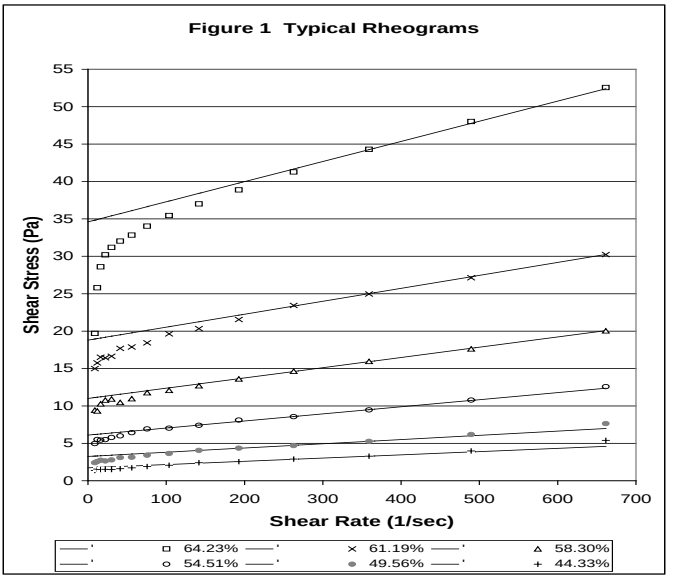

The shear rates shown in Figure 1 and used in all analyses in this paper, are the shear rates applicable to a Newtonian fluid, as supplied by the instrument manufacturer, and no attempt has been made to determine the true shear rate. This simplification is justified by the narrow 1.29 mm gap and diameter ratio close to unity and is in keeping with normal slurry pipeline engineering practice.

3.3 Slurry viscosity components and proposed method of determining the inherent viscosity

It is generally found that plastic viscosity measurements of a slurry at various concentrations are well correlated by the following equation.

$$\mu_{tot} / \mu_w = e^{A_{tot}\, Vrt} \qquad (2)$$

where μ_{tot} = plastic viscosity of the total slurry
μ_w = viscosity of water at the same temperature
A_{tot} = Correlating constant
Vr_{tot} = Volume ratio of total solids = $Cv_{tot} /(1-Cv_{tot})$
Cv_{tot} = volume fraction of total solids

It is now assumed that μ_{tot} is made up of an "inherent" viscosity, μ_{inh}, times a "mechanical interference" component, μ_{mi}, where μ_{inh} is considered an inherent property of the slurry existing even when the slurry is static, and is generally due to surface chemical effects.

$$\mu_{tot} = \mu_{inh} \cdot \mu_{mi} \quad (3)$$

As previously noted, the plastic viscosity of most slurries can be expressed as an exponential function of Volume Ratio of solids. Therefore the inherent viscosity portion is given by:

$$\mu_{inh} / \mu_w = e^{Ainh\ Vrinh} \quad (4)$$

where Vr_{inh} = Volume Ratio of "inherent" solids in the "inherent" slurry
= "Inherent" solids volume/Water volume, i.e.

$$Vr_{inh} = Cv_{inh} / (1-Cv_{inh}) \quad (5)$$

Let β = fraction of "inherent" solids in the total solids. (In a clay-sand slurry mixture, β = volume clay solids/volume total sand plus clay solids). Then Eqn 5 can be rewritten as Vr_{inh} = Clay solids volume / Water volume, i.e.

$$Vr_{inh} = \beta\ Cv_{tot} / (1-Cv_{tot}) = \beta\ Vr_{tot} \quad (6)$$

Therefore, in terms of the Volume Ratio of total solids Eqn 4 becomes:

$$\mu_{inh} / \mu_w = e^{Ainh\ \beta\ Vrtot} \quad (7)$$

With a wide size distribution slurry β is not known so we are normally interested in expressing μ_{inh} directly in terms of Vr_{tot} therefore Eqn 7 is rewritten as:

$$\mu_{inh} / \mu_w = e^{Atinh\ Vrtot} \quad (8)$$

$$\text{where } A_{tinh} = A_{inh}\ \beta \quad (9)$$

Let us now turn our attention to μ_{mi} in Eqn 3. μ_{mi} is an additional viscosity component due to mechanical interference effects between particles in a moving slurry and best described by the previous Eqn 1. It turns out that Eqn 1 is closely approximated by an exponential function of Volume Fraction solids of similar form to Eqn 4, with A_{mi} = 2.7 as seen in Table 1.

Table 1

Vr	.01	0.1	0.2	0.3	0.4	0.5	0.6	0.7	0.8	0.9	1.0
Cv	0.010	0.091	0.167	0.231	0.286	0.333	0.375	0.412	0.444	0.474	0.500
Eqn 5	1.03	1.32	1.74	2.24	2.85	3.64	4.73	6.27	8.46	11.54	15.75
A Av. **2.696**	2.854	2.797	2.767	2.685	2.617	2.584	2.590	2.623	2.670	2.717	2.757

Therefore:

$$\mu_{mi} / \mu_w = e^{Ami\ Vrmi} = e^{2.7\ Vrmi} \quad (10)$$

Combining Eqns 4 and 10, Eqn 3 is rewritten as:

$$\mu_{tot} / \mu_w = e^{Atinh\ Vrtot} \cdot e^{2.7\ Vrmi} \quad (11)$$

Vr_{mi} cannot be expressed as a simple function of β and Vr_{tot}. In Eqn 11, Vr_{mi} is based on the concentration of the coarser solids only. e.g. for a sand-clay slurry Vr_{mi} is based on the concentration of the sand in the slurry. For a wide size distribution slurry we do not know the split between "coarse" solids and "inherent" solids. To overcome this it is now postulated, as an approximation, that <u>all</u> solids, both "coarse" and "inherent", contribute to the mechanical interference component of the viscosity. With this assumption Eqn 11 is rewritten in terms of Vr_{tot} rather than Vr_{mi}.

$$\mu_{tot} / \mu_w = e^{A_{tinh}\, Vr_{tot}} . e^{2.7\, Vr_{tot}} \qquad (12)$$

After combining Eqns 2 and 12 we get;

$$A_{tinh} = A_{tot} - 2.7 \qquad (13)$$

It is recognised that applying Eqn 13 to Eqn 8 to determine μ_{inh} is the same as dividing μ_{tot} by Eqn 1. However Eqn 13 expresses it more elegantly and will also prove helpful when considering the data bank results in Section 4.

The procedure to determine the inherent viscosity therefore becomes:

(a) Conduct viscometer tests over a range of concentrations and determine the plastic viscosity at each concentration in mPas.
(b) If the test temperature is other than 20^0C, normalise the plastic viscosities to 20^0C by assuming the plastic viscosity varies with temperature in the same manner as the water viscosity varies with temperature. e.g. if tested at 25^0C the measured plastic viscosity is multiplied by 1.12.
(c) Graph the normalised plastic viscosities versus Vr_{tot} , including the 1 mPas viscosity of water at zero solids concentration. Fit an exponential trend line to the data. The trend constant equals A_{tot}.
(d) Subtract 2.7 from A_{tot} as per Eqn 13 to get A_{tinh}.
(e) Use Eqn 8 to determine the inherent viscosity for any total solids concentration.

Note: If coarse particles with a high settling rate make testing difficult at (a), the slurry can be scalped to give a finer top size slurry for which testing is manageable. The inherent viscosity determined for the scalped slurry also applies to the original coarser slurry once allowance is made for the differing total concentration. See later Tables 3 and 4 examples.

Figure 2 illustrates a typical result showing the measured plastic viscosity, μ_{tot} (normalised to 20^0C) versus Vr_{tot}. The data are for a coal tailings with p_{50} 25 μm and p_{80} 220 μm. The $R^2 = 0.991$ value shown equals the median R^2 value of all 201 slurries in the data bank to be discussed later in Section 4, so 100 of the slurries in the data bank have a better fit than shown in Figure 2.

The fitted exponential constant 7.719 shown, equals A_{tot} for this slurry. Subtracting 2.7 gives $A_{inh} = 5.019$. The solids SG is 2.12 so for a weight concentration of say 42%, volume concentration is 0.255, and $Vr_{tot} = 0.342$. Total viscosity using $A_{tot} = 7.719$ is 14.0 mPas. The inherent viscosity using $A_{inh} = 5.019$ is 5.56 mPas, i.e. 40% of the total viscosity. The 5.56 mPas inherent viscosity should be used in predicting the turbulent flow deposit velocity rather than the measured 14 mPas.

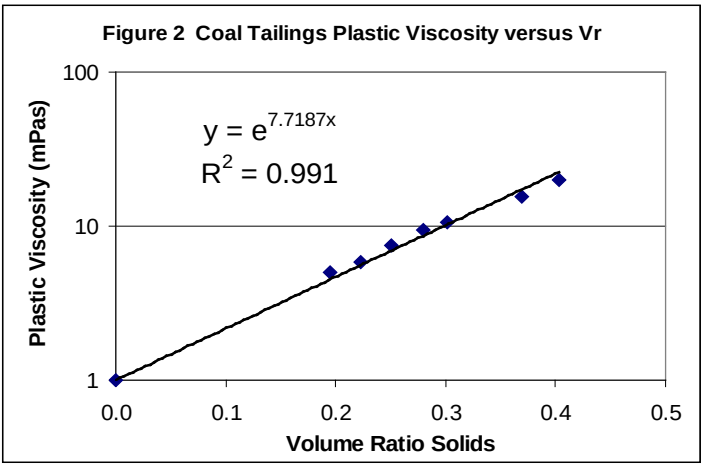

3.4 Some examples illustrating applicability of the method

3.4.1 Applicability of method illustrated by results for sand-clay mixtures

Sand-clay slurry mixtures can be used to illustrate the applicability of the method if it is assumed the plastic viscosity of the clay slurry represents the inherent portion of the total plastic viscosity of the sand-clay mixture. Results are considered for two clay slurries with sand added in two different ratios. These slurries are tailings from a heavy mineral sand project consisting of fines (predominantly clays) mixed with sand. Viscometer tests were conducted on the fines slurry alone and also with the sand added. The results do not form part of the 201 slurries in the data bank because the exact particle size of the fines portion is not known although typically the fines have 99% minus about 75 μm and a p_{50} of around 3 μm. Two different fines were tested, each with two different sand:fines ratios of 79:21 and 90:10 (dry solids basis). The sand added to each of the two fines had different sizes. The sand and fines had similar solids SG 2.67.

For the first slurry, tests on the fines alone at various concentrations gave A_{inh} = 24.04. Additional tests with sand in the ratio 79 parts sand to 21 parts fines solids (dry solids basis) gave A_{tot} = 7.235. Based on the A_{tot} for the mixture Eqn 13 gives A_{tinh} = 4.535 for the inherent (clay) portion. The measured A_{inh} for the clay alone is translated to A_{tinh} for the mixture using Eqn 9 with β = 0.21, giving A_{tinh} = 24.04 x 0.21 = 5.05. The value of A_{tinh} = 5.05 derived from tests on the clay alone is to be compared with the A_{tinh} = 4.535 determined from tests on the mixture. i.e. if no tests were conducted on the clay alone and tests were conducted only on the mixtures the A_{tinh} predicted for the inherent viscosity is within 10% of the "true" A_{tinh}.

For a total weight concentration of 50%, Cv_{tot} = 0.272 and Vr_{tot} = 0.374, giving a total mixture plastic viscosity of 15 mPas. Based on the mixture tests only (A_{tinh} = 4.535) the predicted inherent viscosity is 5.54 mPas. The "true" inherent viscosity (based on A_{tinh} = 5.05) is 6.61 mPas. Further tests were conducted on the same clay slurry and sand with sand:fines ratio 90:10. For both the 79:21 ratio and 90:10 ratio mixture tests the predicted inherent viscosity are within about 20% of the "true" inherent viscosity determined from tests on the fines alone.

A similar series of tests were conducted on a more viscous fines slurry with A_{inh} = 38.7 and also with addition of a coarser sand. Similar accuracies in predicting the inherent viscosity were obtained. The two sets of results are compared in detail in Table 2. In particular the predictions for A_{tinh} by the two different methods shown in **bold** should be compared as well as the resulting inherent viscosity predictions also shown in **bold**. Given the general difficulties in testing slurries, the similarities in the predicted inherent viscosities is considered acceptable and the test results support the method of determining the inherent viscosity of a slurry.

Table 2
Prediction Comparisons Mixtures of Sand in Fines

	Fines 1 A_{inh} = 24.04		Fines 2 A_{inh} = 38.7	
Particle Size of Sand Added (μm)				
P_{80}	320		580	
P_{50}	220		400	
p_{20}	145		200	
From Tests on Fines Alone				
Fraction fines in mixture (dry solids basis), β	0.21	0.10	0.21	0.10
A_{tinh} from tests on fines = β x A_{inh}	**5.048**	**2.404**	**8.127**	**3.870**
From Tests on Mixture				
A_{tot} from tests on mixture	7.235	5.636	10.41	6.626
A_{tinh} predicted from tests on mixture = A_{tot}–2.7	**4.535**	**2.936**	**7.710**	**3.926**
Predictions for 50% Concentration by weight				
(Cv_{tot} = 0.272, Vr_{tot} = 0.374)				
Viscosity of mixture at 50% wt (from A_{tot}),mPas	15	8.23	49.1	11.9
Predicted inherent viscosity from mixture tests	**5.54**	**3.00**	**17.9**	**4.34**
"True" inherent viscosity from tests on fines	**6.61**	**2.46**	**20.9**	**4.25**

3.4.2 Applicability of method illustrated by results for wide size distribution slurries

Another method of testing the suitability of the method of determining the inherent viscosity utilises tests on wide size distribution slurries. First consider rheology test results for a magnetite slurry (SG 4.86). The original magnetite slurry was minus 300 μm with p_{80} 97 μm and p_{50} approximately 44 μm. (actual sizing 50.9% minus 45 μm). Rheology tests were able to be conducted on the minus 300 μm slurry with no scalping required. To provide evidence of the suitability of the proposed method of determining the inherent viscosity, some of the slurry was wet screened at 45 μm and the minus 45 μm fraction collected and concentrated and then also tested separately.

Assuming that the inherent viscosity is due to particles finer than 45 μm then the inherent viscosity of both the minus 300 μm and minus 45 μm slurries should be the same. i.e. both slurries will be made up of the same inherent portion with differing additional coarser mechanical interference components.

The plastic viscosity results for both slurries were each correlated using Eqn 2, giving A_{tot} = 4.44 for the minus 300 μm slurry and A_{tot} = 5.83 for the minus 45 μm slurry. Subtracting 2.7 from each we get A_{tinh} = 1.74 for the minus 300 μm slurry and A_{tinh} = 3.13 for the minus 45 μm slurry. The results are compared in Table 3. The first bordered column shows the predicted inherent viscosity for various concentrations tested, predicted from the minus 300 μm rheology. The second bordered column shows the predicted inherent viscosity

predicted from the minus 45 μm concentrations in the total slurry. The predicted inherent viscosities agree within about 10%.

Table 3

Calculating inherant viscosity of minus 300 micron slurry					**Calculating inherant viscosity of minus 45 micron slurry**				
Cw total			e^4.44Vr	e^1.74Vr				e^5.83Vr	e^3.13Vr
Cw	Cv	Vr	Total viscosity	Inherent	Cw-45M	Cv-45M	Vr-45M	-45M total viscosity	-45M Inherent
77.21	0.411	0.697	22.09	3.36	63.28	0.262	0.355	7.90	3.03
75.81	0.392	0.645	17.52	3.07	61.45	0.247	0.328	6.77	2.79
73.92	0.368	0.583	13.32	2.76	59.04	0.229	0.297	5.64	2.53
71.35	0.339	0.512	9.73	2.44	55.88	0.207	0.261	4.57	2.26
68.43	0.308	0.446	7.24	2.17	52.44	0.185	0.227	3.75	2.03
64.75	0.274	0.378	5.36	1.93	48.30	0.161	0.192	3.07	1.83

Similar tests have been conducted on a number of other wide size distribution slurries, with tests on the original slurry and then on a finer slurry after screening. The predicted inherent viscosities based on the original slurry and the screened slurry, for the highest and lowest concentrations tested, are shown in the last two columns of Table 4. A comparison of the predictions in these two columns provides a gauge of the accuracy of the method of predicting inherent viscosity.

Table 4
Additional Examples of Inherent Viscosity Prediction
Based on Tests on Wide Size Distribution Slurries and Additional Tests after Screening

Description of Original and Screened Slurries Tested	Highest & Lowest Concs Tested Original Slurry	Total Measured Viscosity of Original Slurry	Predicted Inherent Viscosity based on Original Slurry	Predicted Inherent Viscosity based on Screened Slurry
Silica, minus 600 μm	67.78	26.4	3.10	3.88
(also screened at 75 μm)	58.09	8.65	2.11	2.44
Nickel laterite,minus 600μm	41.26	24.6	13.0	13.7
(also screened at 425 μm)	26.34	5.11	3.69	3.78
Same nickel laterite as above	41.26	24.6	13.0	10.9
(also screened at 212 μm)	26.34	5.11	3.69	3.38
Magnetite, minus 425 μm	78.97	43.4	5.43	2.70
(also screened at 45 μm)	68.45	8.83	2.66	1.77
Same as above,demagnetised	79.57	31.2	3.62	2.57
(also screened at 45 μm)	76.46	17.6	2.92	2.20
Lithium ore, minus 600 μm	69.84	79.1	7.67	4.39
(also screened at 75 μm)	54.66	9.73	2.89	2.16

3.5 Application of predicted inherent viscosity to pipeline predictions

The aim of the present paper is orientated to a means of predicting turbulent flow behaviour and the relevant viscosity required. When designing a slurry pipeline, a major parameter required to be predicted is the deposit velocity. In Section 2 it was argued that the inherent viscosity is the appropriate viscosity to use when predicting the heterogeneous deposit velocity. To obtain the inherent viscosity it is recommended A_{tot} be determined

from tests on the slurry, then A_{tinh} be determined using Eqn 13 enabling the inherent viscosity to be predicted using Eqn 8. The yield stress should also be used to predict the laminar-turbulent transition velocity to determine whether deposition is controlled by transition rather than heterogeneous effects.

The homogeneous pressure gradient will normally be predicted using the total measured viscosity with yield stress included to allow for non-Newtonian effects. The method of Wilson and Thomas (1), or Thomas and Wilson (7) for rough wall, are suitable methods. In addition the inherent viscosity can be used to predict any heterogeneous effects on pressure gradient which might overide the homogeneous prediction.

4. DATA BANK OF RHEOLOGY TEST RESULTS

4.1 Rheology data bank results for 201 different slurries

The second section of this paper presents results from a rheology data bank from tests on 201 different slurries. Over the past 25 years the author has conducted rheology tests on hundreds of different slurries. Test results for those slurries for which complete slurry properties such as particle size, solids SG, pH etc are known, have been assembled into a rheology data bank which currently contains results for 201 different slurries, (56 concentrates, 111 tailings and 34 ores) for slurries from Australia, Chile, Fiji, Indonesia, Iran, New Caledonia, Pakistan and Papua New Guinea. The data bank includes results for concentrates of washed coal, copper, hematite, lead, magnetite (both magnetised and demagnetised) and zinc. Tailings include coal, copper, diamond, flyash, gold, iron, lead, nickel, uranium, and zinc. Ores include bauxite, raw coal, copper, gold, magnesite, nickel, and phosphate.

4.2 Plastic viscosity results from data bank

For each slurry the measured plastic viscosity at various solids concentrations has been correlated with Vr_{tot} as in Figure 2 and the value of A_{tot} determined. The particle size distribution is recorded and characterised in terms of p_{80}, p_{50}, and p_{20} as well as calculated mean particle size. Other data include solids SG and pH.

The determined value of A_{tot} for each slurry has been plotted against various parameters including p_{80} and p_{20} but the simplest and most effective was found to be against the p_{50} particle size. Figure 3 shows A_{tot} versus p_{50} particle size for all 201 slurries grouped into the three populations; Ores, Tailings and Concentrates. Power law trend lines have been fitted to each data set with the Power law equation shown. As would be expected the concentrates exhibit the lowest viscosity, (lowest value of A_{tot}), since any clays have been removed from the concentrates. Clays may be present in the ores and also in the tailings and so the ores and tailings will generally be more viscous than the concentrates. The ore data include some nickel laterite ores which are very viscous, resulting in the power law trend fit to the Ores giving the highest value of A_{tot}.

The goodness of fit for the fitted Power law trend curves are: Concentrates – mean deviation from the trend line, 13.4%, with 82% of data points within one standard deviation; Tailings – mean deviation, 25.7%, with 80% of data points within one standard deviation; Ores – mean deviation 26.0%, with 79% of data points within one standard deviation.

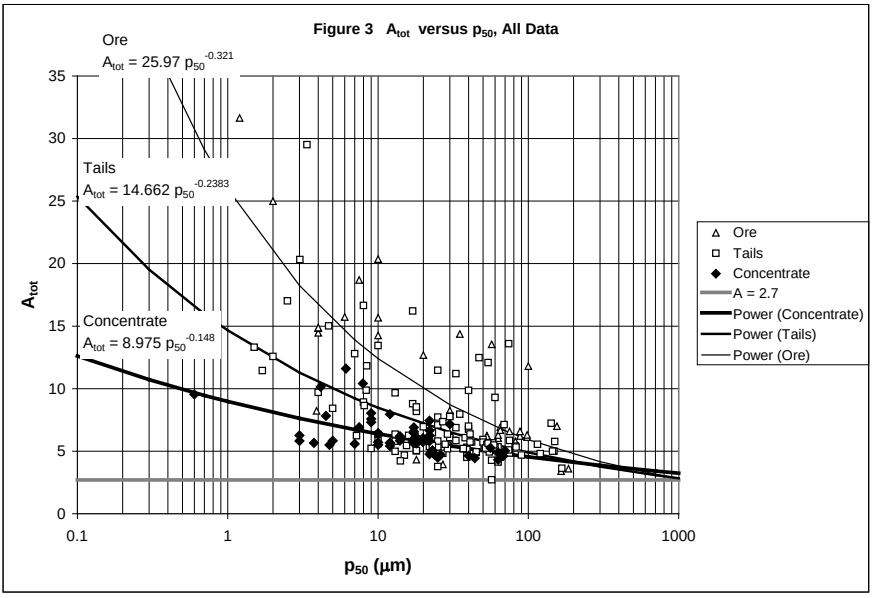

The horizontal grey line in Figure 3 is at A_{tot} = 2.7 which is the value of A applicable to the D.G. Thomas (3) equation (Eqn 1) for the increase in viscosity due to mechanical interference effects as previously seen in Table 1. The fitted Power Law trend lines in Figure 3 approach A_{tot} = 2.7 at around p_{50} = 1000 μm at which p_{50} particle size the 50% of particles finer than 1000 μm will contain almost no particles sufficiently fine to be affected by surface chemical effects and only mechanical interference effects are likely to apply. Note: The Power Law trend lines in Figure 3 have not been forced to approach A_{tot} = 2.7 at around p_{50} = 1000 μm, that is just the trend result from the three sets of data. Figure 3 shows A_{tot} increasing above 2.7 as the particle size decreases and surface chemical effects become more important.

To allow a better gauge of the degree of scatter in the data, the concentrate data points are shown in bold. To further gauge the effect of the scatter in the Concentrate data consider the Concentrate trend line at p_{50} = 10 μm. The trend equation gives A_{tot} = 6.38 and therefore A_{tinh} = 3.68. Considering the 13.4% mean deviation above and below the trend curve at p_{50} = 10 μm, gives A_{tot} ranging from 5.53 to 7.24, giving A_{tinh} ranging from 2.83 to 4.54. For a typical Vr_{tot} = 0.5, the total viscosity based on the trend line is 24 mPas with a range based on 13.4% mean deviation from the trend curve, of 16 to 37 mPas. The inherent viscosity from the trend line is 6.3 mPas with a range based on the 13.4% mean deviation, from 4.1 to 9.7 mPas. For both the total and inherent viscosities the mean range about the trend line prediction is +55%, -35%. For Vr_{tot} = 0.7 the mean range in predicted viscosities increase to +82%, -45%, while for Vr_{tot} = 0.3 they reduce to +29%, -23%. Similar calculations for Concentrate with p_{50} = 100 μm and Vr_{tot} = 0.5, give, for both the total and inherent viscosities, a mean range about the trend line prediction of +35%, -26%. Given the range of different concentrate materials and countries involved (see Section 4.1), the relatively small degree of scatter for the concentrates can be considered remarkable.

4.3 Yield stress from data bank

Yield stress results are also recorded in the data bank. D.G. Thomas (8) found that for seven different slurries with mean particle sizes in the range 0.35 to 13 μm, the yield stress, τ_y, varied with the cube of volume concentration solids, Cv, as in Eqn 14. He also incorporated a term involving particle shape factor but this is not included in Eqn 14 because particle shape has not been measured for any of the slurries in the data bank. D.G. Thomas' equation also included a term with τ_y varying inversely with the square of the mean particle size. This is not included in Eqn 14 but is commented on later.

$$\tau_y = N\ Cv^n \qquad (14)$$

The present author, Thomas (2), showed how addition of "granular", non-colloidal solids, increased the exponent n from 3 to sometimes above 10 as well as resulting in the data following a curved path on a log-log plot of τ_y versus Cv rather than a straight line. Based on Eqn 14, Figure 4 shows the value of the n for all 201 slurries in the data bank plotted against p_{50} particle size. Because the τ_y versus Cv data actually follow a curved path, the fitted value of n is only a mean approximation. Although there is an extremely large degree of scatter, partly for the reasons discussed above, the trend of the data shows n increasing as particle size increases, in agreement with the effect of a greater proportion of coarser non-colloidal particles as per Thomas (2).

Knowing the relative proportion of colloidal (clay) solids and non-colloidal "granular" solids, Thomas (2) developed an expression for yield stress based on applying Eqn 14 to the colloidal solids and multiplying by an expression similar to Eqn 1 based on the proportion of "granular" solids. However this approach cannot be applied to the wide size distribution slurries of interest here because the proportion (β) of solids considered colloidal (or inherent), and the proportion (1- β) of "granular" particles is not known.

As an approximation, the "inherent" portion of the yield stress is assumed given by Eqn 14 with Cv based on the <u>total</u> solids and with n=3. Also, as was the case in regard to Eqn 12, the term $e^{2.7\ Vrtot}$ is included to account for the effects of mechanical interference to give Eqn 15.

$$\tau_y = B.\ Cv_{tot}^{\ 3}\ .\ e^{2.7\ Vrtot} \qquad (15)$$

For fine particle slurries D.G. Thomas (8) found that a log-log plot of τ_y versus Cv had a slope of 3. Because of the fine particle size, the maximum Cv value of his data was 0.25, with Cv for most data considerably less. For coarser slurries, as the p_{50} particle size increases, higher values of Cv are possible. It is found that the $e^{2.7\ Vrtot}$ term in Eqn 15 causes the slope of the log-log plot of τ_y versus Cv_{tot} to increase above 3 and also bends the plot, both effects in keeping with predictions and observations of Thomas (2).

The parameter B in Eqn 15 has been determined for each concentration tested for each slurry and the average value of B determined for each slurry. Typically the upper and lower values of B for any one slurry vary by about +/- 50% from the average value of B over the tested concentration range. The average value of B for each slurry is shown plotted against p_{50} in Figure 5.

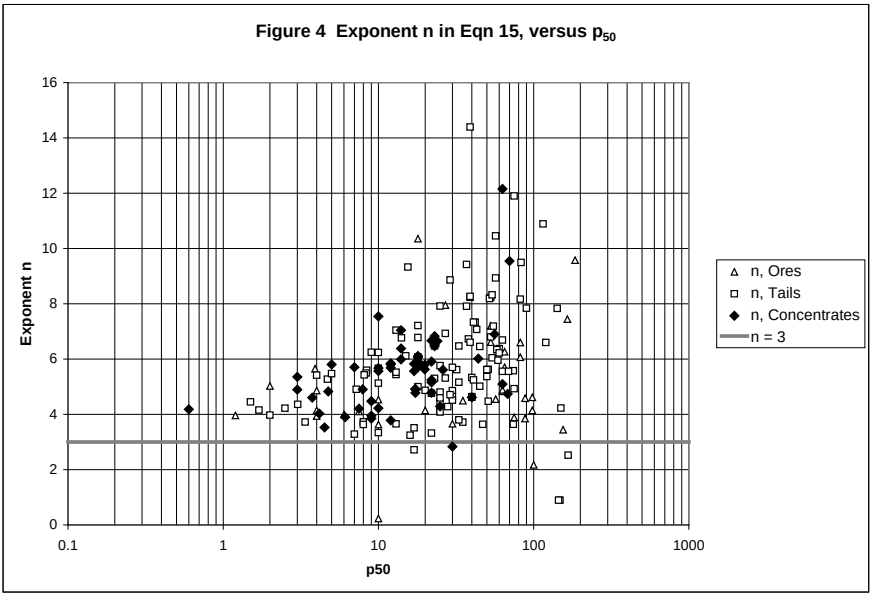

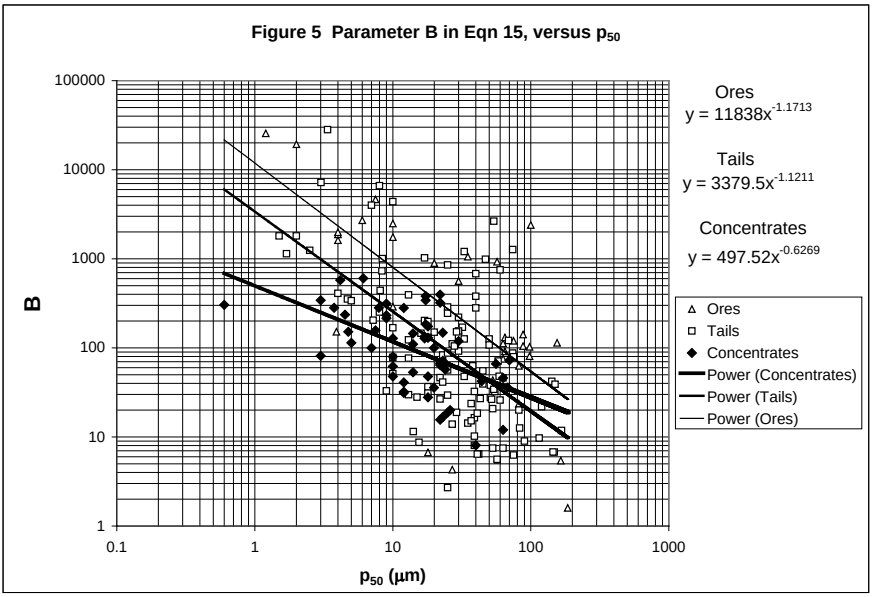

In Figure 5 the mean deviation from the Concentrates trend line is 78% which is much greater than the 13.4% mean deviation for the plastic viscosity in Figure 3. The mean deviation for Tails in Figure 5 is 325% compared with 25.7% for plastic viscosity in Figure 3, and for Ores 255% compared with 26% for plastic viscosity. Because of the very large amount of scatter in Figure 5, especially for the Tails and Ores, the trend lines in Figure 5 can only be used to provide a rough guide as to the likely order of magnitude of yield stress if based solely on particle size.

Note that the steepest trend line slope in Figure 5 is -1.17 which is lower than the -2 slope found by D.G. Thomas (8) mentioned previously in relation to Eqn 14, although his data were limited to a maximum mean particle size of 13 μm.

4.4 Factors Affecting Plastic Viscosity and Yield Stress

In Figures 3, 4 and 5 the plastic viscosity and yield stress have been graphed against p_{50} particle size. It is realised that the p_{50} size does not fully characterise a slurry since a narrow particle size distribution slurry and a very wide size distribution slurry may have the same p_{50} but might be expected to have different rheology, although to some extent the effect of the greater proportion of finer particles in the wide size distribution slurry will be countered by the greater proportion of coarser particles. Various attempts have been made to incorporate particle size distribution. For example in Figure 3 A_{tot} has been graphed against p_{20} and also p_{50} with the ratio p_{80}/p_{20} as parameter. However there is too much scatter to allow realistic trends to be obtained. Further attempts to take into account the particle size distribution will be investigated in the future. Another cause of the scatter is likely to be differences in particle shape and void ratio but neither particle shape or void ratio has been measured for these slurries. More detailed investigations should incorporate a measure of particle shape and/or void ratio if possible.

The yield stress results show much more scatter than the plastic viscosity results. This is because yield stress is influenced much more by the slurry pH and other parameters than is the plastic viscosity. For example the same slurry at two different pH levels could have similar plastic viscosities but quite different yield stress values. The amount of scatter could be reduced by including pH as an additional parameter. With some slurries, prolonged agitation may thicken or thin the slurry. These changes in the slurry consistency are usually due to changes in the yield stress whereas the plastic viscosity is relatively unaffected by the agitation. Magnetite slurries are a special case for which demagnetising the slurry reduces the yield stress but has little effect on the plastic viscosity. Some demagnetised magnetite slurries are included in the data bank. “Viscosity” modifiers, which are sometimes used to thin a viscous slurry, also normally only affect the yield stress rather than the plastic viscosity, although no results with viscosity modifiers are included in the data bank.

5. CONCLUSIONS

After considering turbulent flow prediction methods used for sand-water, sand-brine and sand-clay slurries, it is argued that the plastic viscosity of slurries consists of an inherent component and a mechanical interference component and that only the inherent viscosity should be used to predict the deposit velocity in turbulent flow. A method of determining the inherent viscosity, suitable for practical pipeline design, is presented which does not rely on selecting a demarcating particle size for the vehicle portion of the slurry. The method involves some approximating assumptions but is not intended to be a rigorous analysis of slurry rheology. Instead it is intended to provide a logical approach to turbulent flow prediction and pipeline design.

By considering tests on granular particles in clay slurries and tests on wide size distribution slurries before and after the screening out of coarser particles, the method is shown to give realistic values for inherent viscosity. Plastic viscosity results in a data bank of tests on 201 different slurries are used to illustrate the variation in total plastic viscosity with p_{50} particle size and the inherent viscosity portion. The 201 slurries in the data bank are separated into Concentrates, Tails and Ores, and trend lines fitted to both the plastic viscosity and the yield stress. The trend lines enable estimates of plastic viscosity and yield

stress to be made, based solely on the p_{50} particle size. The estimates for plastic viscosity exhibit a sufficiently small amount of scatter to provide a useful estimate of the plastic viscosity for pipeline scoping studies prior to rheology testing of an actual sample. The yield stress of a slurry is affected much more by factors such as pH, agitation etc and the trend line equations for yield stress only provide an order of magnitude estimate.

6. NOMENCLATURE

A_{inh}	Viscosity parameter in Eqn 4
A_{mi}	Viscosity parameter in Eqn 10
A_{tinh}	Viscosity parameter in Eqn 8
A_{tot}	Viscosity parameter in Eqn 2
B	Yield stress parameter in Eqn 15
Cv	Volume concentration of solids (fraction)
Cv_{tot}	Volume concentration of total solids (fraction)
N	Yield stress parameter in Eqn 14
p_{80}	Particle size applicable to 80% passing
p_{50}	Particle size applicable to 50% passing
p_{20}	Particle size applicable to 20% passing
Vr	Volume ratio solids = volume solids/volume fluid
Vr_{inh}	Volume ratio inherent solids, Eqn 5
Vr_{tinh}	Volume ratio inherent solids, Eqn 13
Vr_{tot}	Volume ratio total solids
β	Fraction of “inherent” solids in total solids
μ_{slurry}	Viscosity (plastic) of slurry, (mPas)
μ_{fluid}	Viscosity of fluid, (mPas)
μ_{inh}	Inherent viscosity (plastic) of slurry, (mPas)
μ_{tot}	Total viscosity (plastic) of slurry, (mPas)
μ_w	Viscosity of water, (mPas)
τ_y	Yield stress, (Pa)

7. REFERENCES

1. WILSON, K.C. and THOMAS, A.D. (1985). A New Analysis of the Turbulent Flow of Non-Newtonian Fluids, *Can. Jnl Chem. Engnr, Vol. 63, August 1985.*

2. THOMAS, A.D. (1999). The Influence of Coarse Particles on the Rheology of Fine Particle Slurries, *Rheology in the Mineral Industry II, United Engineering Foundation, USA, Turtle Bay, Hawaii, March 1999.*

3. THOMAS, D.G. (1965). J. Colloid Sci., 20, p267

4. GILLIES, R.G. and SHOOK, C.A. (1991), “A deposition velocity correlation for water slurries”, *Can. J. Chem. Eng.* ***69****, 1225-1227 (1991).*

5. WILSON, K.C., ADDIE, G.R., SELLGREN, A., and CLIFT, R. Slurry transport using centrifugal pumps, (2nd edn), *Blackie, London, U.K., 1997.*

6. SELLGREN, A. and WILSON, K.C., Validation of a four-component pipeline friction model, *Proc. Hydrotransport 17, Cape Town, South Africa, May 2007. (BHR).*

7. THOMAS, A.D. and WILSON, K.C. (2007). Rough-wall and turbulent transition analyses for Bingham plastics. *Hydrotransport 17 Conference, Cape Town, South Africa. (BHR).*

8. THOMAS, D.G. (1963). Non-Newtonian Suspensions Part 1, Physical properties and laminar transport characteristics. *Ind.&Eng. Chem., Vol 55, No. 11, November, pp 18-29.*